MINISTRY OF EDUCATION AND TRAINING

HO CHI MINH CITY UNIVERSITY OF TECHNOLOGY AND EDUCATION

BUI VAN HIEN

IMPROVING THE EFFICIENCY OF PHOTOVOLTAIC SYSTEMS

PhD THESIS SUMMARY

MAJOR: ELECTRICAL ENGINEERING

Ho Chi Minh City 12/2024

The project was completed at **Ho Chi Minh City University of Tecknology and Education**

Scientific supervisor 1: Associate Professor, PhD TRUONG VIET ANH

Scientific supervisor 2: PhD. NGUYEN VU LAN

Reviewer 1: PhD NGUYEN TRUNG THANG

Reviewer 2: PhD. TRAN THANH NGOC

Ho Chi Minh City University of Tecknology and Education

September 29, 2024

PUBLISHED RESEARCH PAPERS

1. ***Bui Van Hien**, Truong Viet Anh, Nguyen Tung Linh, and Pham Quoc Khanh, "Rapidly Determine the Maximum Power Point in the Parallel Configuration of the Photovoltaic System," Sensors, 2023, 23, 7503.*
2. ***Van Hien Bui**, Viet Anh Truong, Vu Lan Nguyen, Thanh Long Duong, "Estimating the potential maximum power point based on the calculation of short-circuit current and open-circuit voltage," IET Power Electronics, 2024, pp: 1-20.*
3. *Truong Viet Anh, Ton Ngoc Trieu, Pham Vo Hong Nghi, **Bui Van Hien**. "Fast and Accurate GMPPT Based on Modified P&O Algorithm". IEEE Access, Vol 12, 2024, pp: 29588-129600, doi: 10.1109/ACCESS.2024.3457825.*
4. ***Bùi Văn Hiền**, Trương Việt Anh, Quách Thanh Hải (2020). "Tối ưu điểm phát công suất cực đại của pin quang điện làm việc trong điều kiện bóng che". Tạp chí Phát triển Khoa học và Công nghệ – Kĩ thuật và Công nghệ, 73(1):326-338*
5. ***Bùi Văn Hiền**, Nguyễn Tùng Linh, Nguyễn Vũ Lân, Trương Việt Anh, Nguyễn Hồng Nguyên, "Truy Xuất Điểm Phát Công Suất Cực Đại Của Hệ Thống Pin Quang Điện Trong Các Thiết Bị Di Chuyển", Tạp chí Khoa học và Công nghệ Đại học Thái Nguyên 227(08)2022: pp 131 – 139*
6. *Trương Việt Anh, **Bùi Văn Hiền**, Nguyễn Tùng Linh, Nguyễn Vũ Lân, Quách Thanh Hải, "Đề Xuất Giải Pháp Tìm Điểm Phát Công Suất Cực Đại Của Hệ Thống PV Dựa Vào Dự Đoán Giá Trị I_{sc} Và V_{oc}", Tạp chí Khoa học và Công nghệ Đại học Thái Nguyên 227(11):2022, pp 77-86.*
7. *X. T. Luong, **V. H. Bui**, D. T. Do, T. H. Quach and V. A. Truong, "An Improvement of Maximum Power Point Tracking Algorithm Based on Particle Swarm Optimization Method for Photovoltaic System". 2020 5th International Conference on Green Technology and Sustainable Development (GTSD), Ho Chi Minh City, Vietnam, 2020, pp. 53-58*
8. *Trinh Trong Chuong, Nguyen Duc Minh, **Bui Van Hien**, Fan Yang, Truong Viet Anh (2021). "Optimizing the Performance of the Photovoltaic System using the Micro DC-DC Converter". 2021 3rd International Conference on Smart Power & Internet Energy Systems (SPIES) 978-1-6654-3879-7/21/$31.00 ©2021 IEEE*
9. ***Bui Van Hien**, Truong Viet Anh, Nguyen Duc Minh, Trinh Trong Chuong, Y Do Nhu, Trieu Viet Phuong, "Module Integrated Converters and Independent MPPT Technique" International Conference on Engineering Research and Applications, 2022, 685-698*

CHAPTER 1. INTRODUCTION

1.1 Research background

Energy from photovoltaic systems (PVS) is sustainable and available everywhere, reducing environmental impacts, transmission and distribution losses, and using on-site power generation space [1]. However, PV energy harvesting technology faces continuous changes and loss of synchronization during operation, causing energy losses. The two main issues for optimizing PV performance are developing MPPT techniques and adjusting PV configuration to reduce the impact of partial shading conditions (PSC) [2].

- Developing GMPPT techniques to avoid LMPP traps to accelerate convergence, improve efficiency, reduce costs, and maintain stability. Traditional methods are simple and easy to implement but less accurate. In contrast, the group's optimization algorithms and high-performance hybrid solutions are expensive and slow [3].
- Restructuring PVS to control the number of MPPs, reduce the impact of PSC, and improve power extraction efficiency. The series type (SC) faces many extremes when PSC occurs while the parallel type (PC) has one extreme in all conditions, but the large current causes losses on the control circuit. S-PC is widely applied and studied but has the same disadvantages as SC. Improved TCT, BL, and HC forms increase costs and losses on backup links [4], [5], [6].

Therefore, it is necessary to combine the development of the MPPT algorithm and propose a PV configuration to optimize power generation efficiency at the most reasonable cost. Thus, the topic "**Improving the efficiency of Photovoltaic Systems**" researches and develops the GMPPT algorithm for PC and SC or S-PC configurations in PSC to improve energy extraction efficiency from PV systems.

1.2. Objectives of the thesis

The overall objective is to develop MPPT algorithms for PVS under PSC, specifically including:

- Proposing MPPT algorithms for parallel-linked PV systems operating under partial shading conditions.
- Research and propose GMPPT algorithms for SC or S-PC configurations when the PV system operates under PSC.
- Researching, applying, simulating, and analyzing the performance of PVS under the impact of PSC.

1.3. Scope of the thesis

Solutions to improve the performance of PVS based on MPPT techniques for PC and SC or S-PC configurations operating under partial shade conditions.

1.4. Methodologies and approaches

References to relevant sources. Improve, propose, and apply GMPPT algorithms for PVS operating under partial shade conditions.

1.5. Contributions of the thesis

Propose a $0.4V_{oc}$ limit to quickly determine the starting point for the improved P&O algorithm. A solution considering the optimal value of the DC/DC converter to promptly estimate the potential MPP for the PC configuration.

Propose a solution to determine the voltage gap caused by PSC on the SC or S-PC configuration. Develop an LMPP trap avoidance algorithm based on the simulation of the I-V curve of the PV system.

The proposals are applied to increase efficiency, convergence speed, stability, and good dynamic response due to

reducing iteration steps.

1.6. The thesis authenticity

- MPPT solution for parallel PV systems is suitable for small and medium capacity and voltage applications such as rooftop solar power, water pumping systems, traffic lights, and continuously moving devices.
- The GMPPT algorithm, according to PSC, is a simple, effective method with less oscillation due to using few loops. This method can be applied to PV systems connected in series or series - parallel operation under continuously fluctuating radiation and temperature conditions.

1.7. Organization of the thesis

The thesis consists of 5 chapters organized as shown in Figure 1.1.

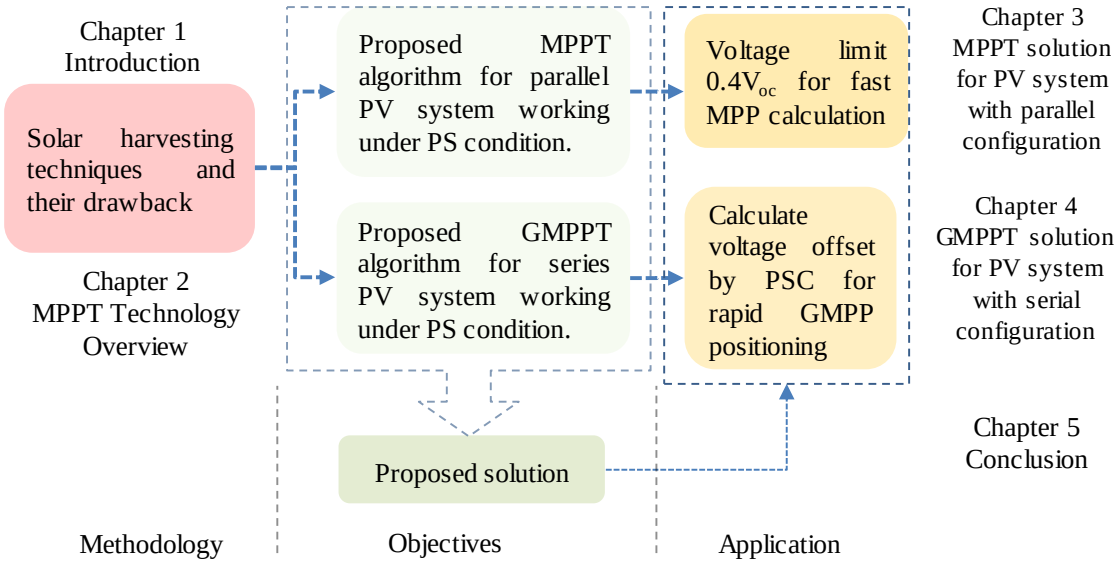

Figure 1.1 Structural diagram of the thesis.

CHAPTER 2. OVERVIEW OF MPPT TECHNIQUE

2.1 Effect of operating conditions on PV characteristics

2.1.1. Characteristics of photovoltaic cells

Operating conditions affect the performance of the PV systems. To distinguish GMPP in many LMPPs, it is necessary to develop algorithms and restructure the PV system to reduce the impact of PSC. The I-V and P-V characteristics of the PV model (Figure 2.1) according to the environment have been studied and investigated. The results presented in Figure 2.2 show that the current I_{sc} is more affected by the irradiation intensity than the voltage value V_{oc}. On the contrary, V_{oc} fluctuates more when the temperature changes [7].

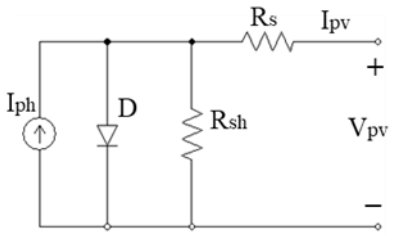

Figure 2.1 PV cell mathematical model.

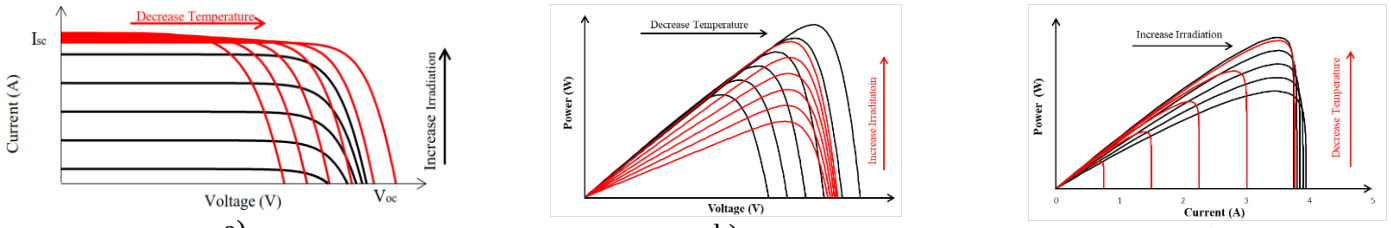

a) b) c)

Figure 2.2 Effect of temperature and radiation on a) I-V; b) P-V; và c) P-I characteristics

2.1.2. Effect of PSC on the PV structures

Investigation of the influence of PSC on the MSX-60 PV module [8] with basic configurations as shown in Figure 2.3.

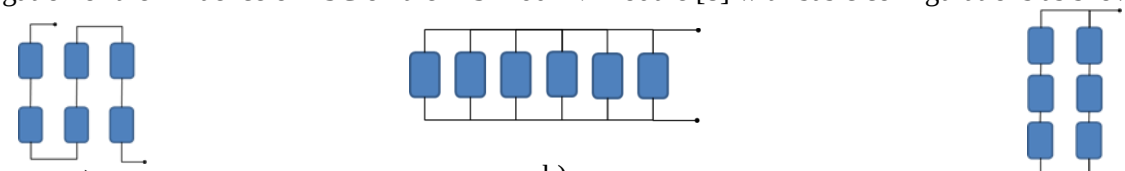

a) b) c)

Figure 2.3 The PV system in a) SC; b) PC; c) S-PC; và d) P-SC.

The survey results under homogeneous conditions and PSC randomly on the configurations show that:

- PC has one extreme and has the most significant power under all operating conditions.
- SC has the most LMPPs.
- SC has the lowest current, and PC has the lowest voltage.

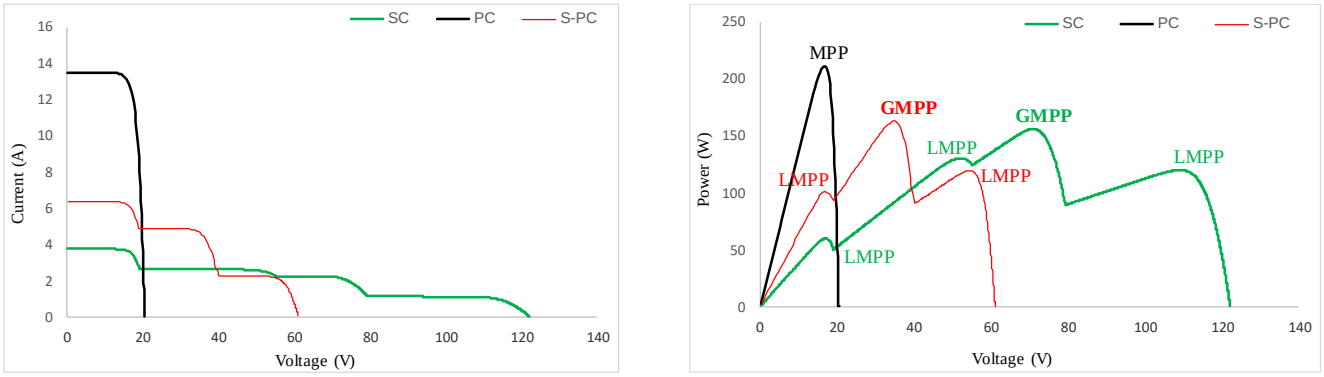

a) b)

Figure 2.4 Comparison of the characteristics under PSC: a) I-V và b) P-V.

Under the influence of PSC, the series configuration (SC) has the following characteristics:

- The number of peaks equals the number of PVs receiving different radiation in the link.
- The Isc value is proportional to the radiation and decreases as the shading level increases.
- $I_{sc,sys}$ of PVS equals the I_{sc} of PV receiving the largest radiation.
- V_{oc} also decreases with radiation but not significantly.
- The GMPP location in the case of PSC is random.
- Uniform operating conditions always produce the largest peak power.

The above conclusions are the basis for effectively reviewing, simulating, and analyzing the operating state of PVS to determine the best operating area.

2.2 Common MPPT techniques

This section examines some of the most popular MPPT algorithms according to the following classification criteria: MPPT speed, control parameters, whether it depends on the PV type, complexity in the design diagram, stability, cost, ability to handle shading, efficiency, and which DC/DC converter is used. According to the above criteria, three groups of algorithms are examined and summarized in Tables 2.2 to 2.4 [9]. Figure 2.15 introduces the classification of some algorithms according to the essential criteria.

Table 2.1. Benchmark comparison of some traditional algorithms.

Parameters	**P&O**	**InC**	**CV**	**CC**
MPPT speed	T	T	T	T
Accuracy	TB	TB	T	T
Control parameters	I, V	I, V	V	I
Dependent on the type of PV	K	K	Yes	Yes
Complexity	T	TB	T	T
Stability	K	PT	K	K
Cost	TB	TB	T	T
PSC Processing	K	K	K	K
Efficiency	98,98	99,94	100,00	99,88
Converter type	Boost	Boost	Boost	Buck-boost
References/year of publication	[10]/2021	[10]/2021	[11]/2017	[12]/2024

Note: T: Low; TB: Medium; K: None; PT: Dependent on PV; KPT: Regardless of PV.

2.3 Chapter summary

PSC is an obstacle to improving the technology of energy extraction from PVS with the following disadvantages:

- PC is simple, but the current on the large switches puts pressure on the controllers
- SC has to solve the multi-pole problem in PSC, making it ineffective in avoiding LMPP trapping and increasing costs.
- The nonlinearity of P-V and I-V characteristics under all operating conditions.
- MPPT efficiency and speed are difficult to achieve simultaneously in the same solution.
- Optimization algorithms depend on population size, so the speed is slow.

The thesis proposes MPPT solutions based on the characteristics of I-V and P-V curves under operating conditions. This is considered a two-stage MPPT solution in which:

- The first stage to limit the potential MPP region is based on simulating the shape of PV characteristics under specific operating conditions to determine the exact LMPP.
- The next stage is to use the traditional MPPT algorithm to exploit simplicity and high speed without sacrificing performance.

Table 2.2. Benchmark comparison of some optimization algorithms.

Parameters	**PSO**	**ABC**	**ACO**	**ANN**	**BA**	**GWO**	**GA**
MPPT speed	C	C	C	TB	C	TB	TB
Accuracy	TB	TB	TB	C	C	C	C
Control parameters	V, I	V, I	V, I	V, I/ G, T	V, I	V	V, I
Dependent on the type of PV	K	K	K	Yes	K	K	K
Complexity	C	C	C	C	C	C	C
Stability	C	C	C	C	C	C	C
Cost	TB	C	TB	C	C	TB	C
PSC Processing	Yes	Yes	Yes	Yes	Yes	Yes	Yes
Efficiency	-	99,8	-	99,81	99,9	99,57	-
Converter type	Boost	Boost	Boost	Boost	Boost	-	Boost
References/year of publication	[13]/2023	[14]/2021	[15]/2021	[16]/2023	[17]/2022	[18]/2024	[19]/2023

Note: C: High; TB: Medium; K: None.

Bảng 2.3. Benchmark comparison of some hybrid algorithms.

Parameters	**ANN-P&O**	**PSO-P&O/InC**	**GWO-ANFIS**	**AFO**
MPPT speed	TB	C	C	TB
Accuracy	C	C	TB	TB
Control parameters	V, I	V, I	V, I	V, I
Dependent on the type of PV	Yes	K	K	K
Complexity	C	TB	TB	C
Stability	C	TB	C	TB
Cost	C	TB	C	C
PSC Processing	Yes	Yes	Yes	Yes
Efficiency	-	98,00	98,20	98,7
Converter type	Boost	Boost	Boost	Boost
References/year of publication	[20]/2024	[21]/2024	[45]/2024	[22]/2024

C: High; TB: Medium; T: Low; K: None.

Based on the above analysis, the thesis will develop a GMPPT algorithm with the following specific contents:

1. Propose a minimum voltage limit to determine the I_{sc} and V_{oc} of the PV system. Combined with survey and analysis to propose the optimal D value for DC/DC converters to measure the two parameters I_{sc} and V_{oc} without interrupting the power supply. This solution has been presented and applied in publications {1}, {2} and {5}.

2. Apply the CV method combined with an improved P&O algorithm to quickly determine the potential MPP by locating the points (0, I_{sc}) and (V_{oc}, 0) on the I-V graph of the PV system in the PC link. The proposed solution is applied in publications {1}, {2}, and {5}.

3. Simulate the I-V characteristics of the SC or S-PC system under PSC to propose the GMPPT algorithm to improve efficiency and convergence speed. The proposed algorithm is also applied in publication {3}, and related works {4}, {6-9}.

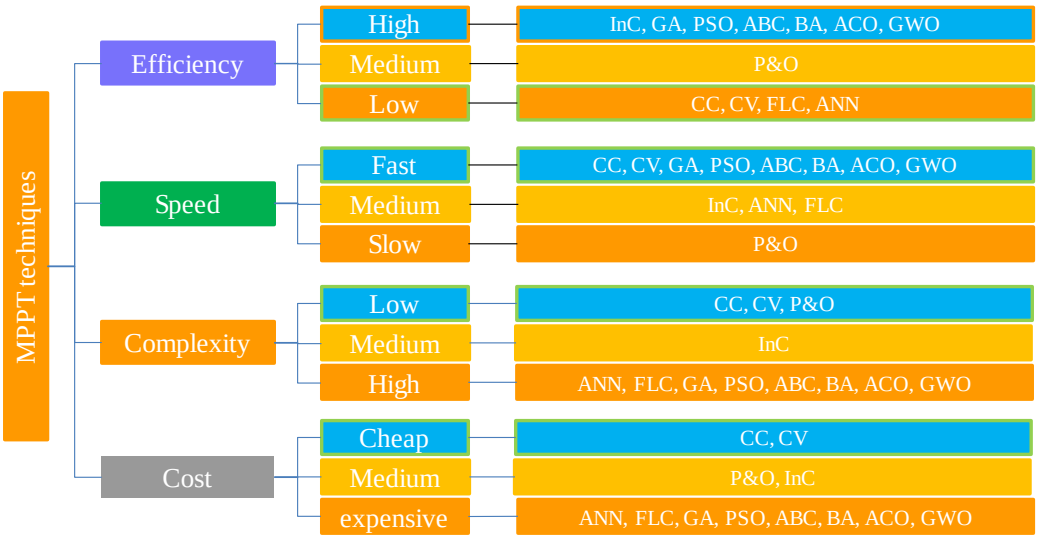

Hình 2.15 Classification of MPPT solutions according to basic criteria [3].

CHAPTER 3

MPPT SOLUTION FOR PV SYSTEM WITH PARALLEL CONFIGURATION

3.1. Research background

The solutions are mainly based on I_{pv}, V_{pv}, and filling factor (FF), which require I_{sc} and V_{oc} of PVS [23]. The CV and CC methods interrupt the power supply, resulting in power loss. To overcome this, the solution of directly determining I_{sc} and V_{oc} according to D is proposed to avoid interrupting the power supply and improve the efficiency of PVS.

3.1.1. Fill factor of some typical PV types

The FF of each PV type is different and changes according to operating conditions. The radiation range from 200W/m^2 to 1000w/m^2 and temperature from 0^{o}C to 60^{o}C were surveyed to determine the relative FF of some typical PV kinds. The results show that the current factor, k_i, is from 0.91 to 0.93, and the voltage factor, k_v, is from 0.75 to 0.8.

3.1.2. The best operating range of DC/DC converters

The thesis examines three DC/DC circuits with K being the ratio between output and input voltage, D being their best duty cycle under the condition that D approaches 0.5 [24]:

$$\begin{cases} K_{Boost} = \dfrac{1}{1-D} \\ K_{Buck} = D \\ K_{Buck\text{-}boost} = \dfrac{D}{1-D} \end{cases} \quad (3.3)$$

Ignoring the losses on the components of the DC/DC converter, the relationship between the input and output power is related to the internal resistance of the PV (R_{in}) and the load resistance (R_L) according to equation (3.7). Within the proposed survey range, the internal resistance of the PV will vary from the lowest value, R_{in_1} (at M_1), to $R_{in\text{-}2}$ (at M_2), as shown in Figure 3.3.

$$R_L = K_{mp1}^2 R_{in\_1} = K_{mp2}^2 R_{in\_2} \quad (3.7)$$

Or

$$\frac{K_{mp1}^2}{K_{mp2}^2} = \frac{k_v V_{oc2}}{k_i I_{sc2}} \frac{k_i I_{sc1}}{k_v V_{oc1}} = \frac{V_{oc2}}{I_{sc2}} \frac{I_{sc1}}{V_{oc1}} \quad (3.9)$$

Where V_{oc} and I_{sc} at T^{o}C temperature and W (W/m^2) irradiation condition are determined according to standard conditions as in (3.10) [25]:

$$\begin{cases} V_{oc} = V_{oc\_ref} - \alpha_v (T - T_{ref}) \\ I_{sc} = \left(I_{sc\_ref} + \alpha_i (T - T_{ref}) \right) W / W_{ref} \end{cases} \quad (3.10)$$

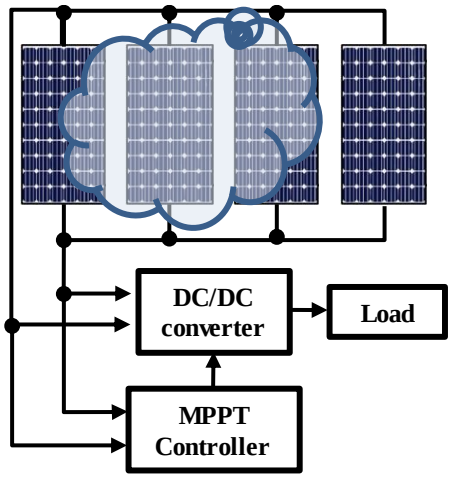

Figure 3.1 Parallel PV system configuration.

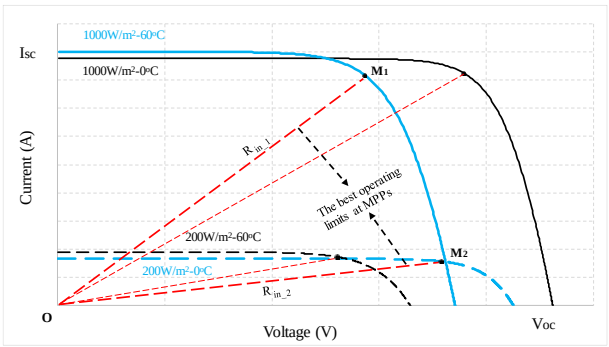

Figure 3.3 Resistance limit in the survey area.

Substituting equation (3.9) into (3.7), we get the relationship between the two MPP positions as follows:

$$K_{mp1} = 2,46 K_{mp2} \quad (3.13)$$

The relationship between duty cycle at two operating points satisfying equation (3.13) is expressed as in (3.14).

$$D_{mp1} = 1 - D_{mp2} \quad (3.14)$$

Combining equations (3.14) with (3.3), the D_{mp1} and D_{mp2} values of the Boost and Buck converters are 0.71 and 0.29; the Buck-boost converter is 0.61 and 0.39. Surveying the remaining PVs, the best operating limits are listed in Table 3.5.

Table 3.5 The best operating limit of D

PV modules	Boost		Buck		Buck-boost	
	D_{mp1}	D_{mp2}	D_{mp1}	D_{mp2}	D_{mp1}	D_{mp2}
MSX-60	0,71	0,29	0,71	0,29	0,61	0,39
Shell SP75	0,64	0,36	0,64	0,36	0,57	0,43
Shell SQ150	0,67	0,33	0,71	0,33	0,59	0,41
SSt 230-60P	0,66	0,34	0,67	0,34	0,58	0,42
Shell S70	0,64	0,36	0,64	0,36	0,57	0,43
GxB-340	0,69	0,31	0,69	0,31	0,66	0,40
Shell ST40	0,60	0,41	0,60	0,41	0,54	0,45

3.2. Proposed method to determine Isc value based on D

In the range from R_{in-1} to R_{in-2}. If $D > D_{mp1}$ (at M_1), then $R < R_{in-1,}$ so the measured current belongs to the linear region, which can be used to calculate I_{sc}. Conversely, if $R > R_{in-2,}$ meaning $D < D_{mp2}$ (at M_2), then it always falls into the nonlinear region used to calculate V_{oc}.

3.2.1. Calculate I_{sc} within the limit of $0,2V_{oc}$

The Isc value, calculated according to [26] at A(V_A, I_A) with $V_A = 0,2V_{oc}$. Substitute the coordinates of two points into equation (3.9) to determine the relationship between A and M_1 for all converters. Then, the results of calculating the value of D at A are listed in Table 3.6 show that:

Table 3.6 The D values of PVs at $0.2V_{oc}$ and $0.4V_{oc}$ correspond to DC/DC converters.

PV modules	$0,2V_{oc}$			$0,4V_{oc}$		
	Boost	Buck	Buck-boost	Boost	Buck	Buck-boost
MSX60	0,86	1,48	0,76	0,80	1,04	0,69
Shell SP-75	0,82	1,33	0,73	0,75	0,94	0,66
Shell SQ-150	0,84	1,42	0,75	0,78	1,00	0,68
SST 230-60P	0,83	1,39	0,75	0,77	0,98	0,67
Shell S70	0,83	1,34	0,74	0,75	0,95	0,66
GxB-340	0,85	1,44	0,75	0,79	1,01	0,68
Shell ST40	0,81	1,25	0,71	0,72	0,88	0,64

- For Boost and Buck-boost converters, the I_{sc} value can be measured at $0,2V_{oc}$.
- For Buck converters, I_{sc} cannot be measured at $0,2V_{oc}$. The closer the D value is to 0 or 1, the more disadvantageous it is for DC/DC converters.

3.2.2. Proposed calculation of I_{sc} at $0,4V_{oc}$

From the mathematical model, Figure 2.1, of PV, using the graph in Figure 3.5 to describe Eq. (3.23) shows that:

$$I_{pv} = I_{sc} - I_D - I_{R_{sh}} \quad (3.23)$$

- The component causing nonlinearity on the I-V curve is I_D
- In range $0 < V_{pv} < xV_{oc}$, the equations are considered linear; the slope of the I-V curve is caused by I_{Rsh}.
- If $V_{pv} > xV_{oc}$, the I-V characteristic starts to be non-linear due to I_D.
- The point separating the two regions is the point that satisfies Eq. (3.26) and reaches its maximum value.

$$f(x) = I_{Rsh} - I_D = \frac{xV_{oc}}{R_{sh}} - I_0\left\{e^{\frac{qxV_{oc}}{nkT_c}} - 1\right\} \quad (3.26)$$

The function f(x) reaches a maximum when it satisfies the condition of equation (3.27).

$$x = \frac{1}{c}\ln\left(\frac{a}{bc}\right) \quad (3.27)$$

$\lambda = 0{,}6x$ is chosen to determine an utterly linear line segment, so the x limit is.

$$x = 0{,}6\frac{1}{c}\ln\left(\frac{a}{bc}\right) \quad (3.28)$$

The linear regions of PV modules are surveyed and summarized in Table 3.7.

The results show that all PV modules are linear in region $V < 0{,}4V_{oc}$, so it is chosen as the limit to calculateI_{sc}. The value of D at A'($0{,}4V_{oc}$, I_{sc}) is calculated similarly to that at A($0{,}2V_{oc}$, I_{sc}); the results are summarized in Table 3.6, showing that.

- The D value at $0.4V_{oc}$ is smaller than that at $0.2V_{oc}$ in all investigated cases.
- I_{sc} can be measured at D > 0.8 for the Boost converter and 0.7 for the Buck-boost converter.
- The D value of the Buck converter at $0.4V_{oc}$ is also more reasonable than that at $0.2V_{oc}$.

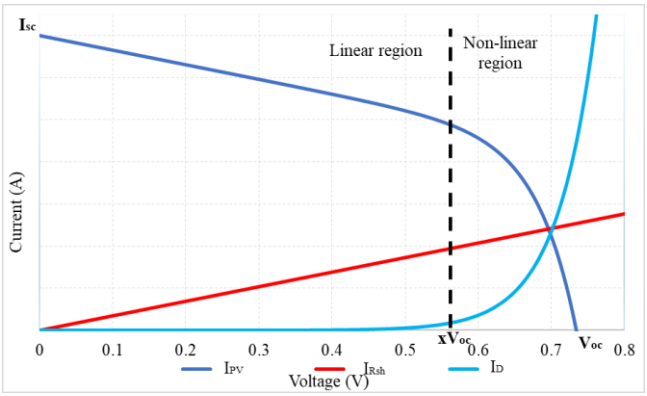

Figure 3.5 Working zones on the I-V curve.

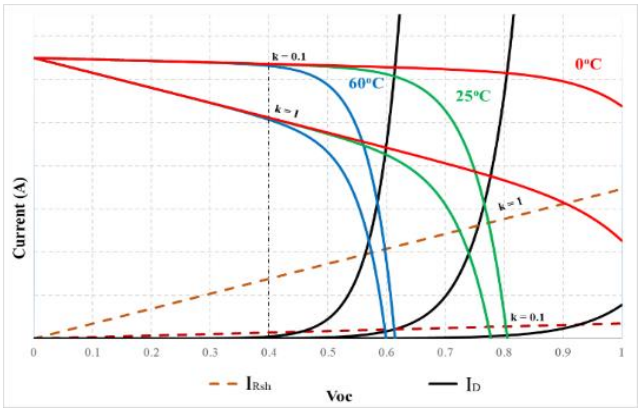

Figure 3.6 Linear limit survey of PV MSX-60.

Table 3.7 Linear region limit on I-V curve.

Parameters	Monocrystalline		Polycrystalline			Thin-film	
	Shell SP75	Shell SQ150	SST 230-60P	Shell S70	MSX-60	GxB-340	Shell ST40
xV_{oc}	0,46	0,48	0,49	0,48	0,47	0,49	0,5

3.2.3. Proposed method for calculating I_{sc}.

From two points $P_1(V_1, I_1)$ and $P_2(V_2, I_2)$ in the region less than $0{,}4V_{oc}$. Calculate the I_{sc} value according to equation (3.34) and check the percentage error.

$$I_{cal} = I_1 - \frac{I_2 - I_1}{V_2 - V_1}V_1 \quad (3.34)$$

For the Boost converter: The largest ΔI% is 2,63%, and the largest average percentage error ($\Delta I\%_{tb}$) is 0,34% and can reach 100%.

The Buck-boost converter also has the largest average error of 0.18% and the largest error of 1.12%.

Buck converter has the largest error of ΔI% = 5,85%, the largest average error of 0.77%, and the smallest average error of 0.13%.

3.3. Solution to determine V_{oc} of PV system

According to [26], the V_{oc} can be calculated from position B(V_{oc}; 0,2I_{sc}). Similar to the survey at A, the value of D at B(V_{oc}; 0,2I_{sc}) is referenced to M2 for calculation for DC/DC circuits with data listed in Table 3.10 showing that:

V_{oc} can be measured at D < 0.1 for the Buck converter and D < 0.2 for the Buck-boost converter. On the contrary, the Boost converter has D < 0, so choose D = 0 to measure V_{oc}. The calculated voltage error when using the proposed parameters is summarized as follows:

The Buck-boost converter has the lowest calculation error of about 0.32%.

The Buck converter has the largest error of 2.31%, the largest average error is about 1.62%, and the smallest average error is only 0.48%.

The Boost converter has the largest average error of about 7.64%, and the lowest average error is 1.72%.

The average error for all the surveyed cases is about 1.52%.

In summary, calculating I_{sc} and V_{oc} directly will reduce the power interruption time and estimate the potential MPP location to increase the power generation efficiency for PVS. This proposed method is used in publications {1-3} and {5}.

Bảng 3.10. The duty cycle value is determined at 0,2I_{sc}.

Parameters	MSX-60	Shell SP75	Shell SQ150	SSt 230-60P	Shell S70	GxB-340	Shell ST40
Boost	-0,71	-0,54	-0,61	-0,59	-0,54	-0,66	-0,42
Buck	0,12	0,15	0,13	0,14	0,15	0,12	0,17
Buck-boost	0,21	0,23	0,22	0,23	0,24	0,21	0,25

3.4. Identify potential MPP locations

The proposed solution uses the starting values in Table 3.12 to estimate the potential MPP locations for the improved P&O (I_P&O) algorithm. The flowchart of the I_P&O algorithm is shown in Figure 3.9.

3.5. Simulation results and evaluation

The PV system, as shown in Figure 3.1, was tested on all three DC/DC converters to evaluate the following results:

3.5.1. Evaluation of Dmp and Pmp values of output algorithms

For the Boost converter, the calculated D_{mp} value of 0.4775 compared to the converged D_{con} = 0.4475 has an error of about 0.03 (Figure 3.10). The value I_{cal} = 6.0159 A coincides with I_{sc} = 6.01. Meanwhile, V_{cal} = 20.17 V has an error of about 1.0% compared to V_{oc} = 19.97 V. As a result, the estimated power waveform with P_{mp} = 90.66 W has an error of about 1.1% compared to the converged value P = 91.66 W.

The calculated D_{mp} value of the Buck converter is 0.38, and the convergence value is at D_{con} = 0.41 (deviation 0.03). Finally, the Buck-boost converter can determine D_{mp} = 0.38 compared to the convergence position of D_{con} = 0.42 with an error of about 0.04 (Figure 3.11).

The summary of the survey results for all the proposed PV types listed in Table 3.13 shows that:

The Boost converter has an average error of 0.07. The power deviation is 12.66%, with an accuracy of up to 99.93%.

The Buck converter has an average error of 0.04. Therefore, the estimated power has an accuracy of up to 99.83%.

The Buck-boost converter has an estimated D error of less than 0.04, with an accuracy of up to 99.96%.

In summary, from the potential MPPs, the P&O algorithm deployed for search helps the overall solution to increase convergence speed and achieve high efficiency due to its ability to limit the search area.

Table 3.12. The starting values of the algorithm.

Parameters	Boost	Buck	Buck-boost
$\mathbf{D_1}$	0,82	1	0,82
$\mathbf{D_2}$	0,80	-	0,80
$\mathbf{D_3}$	0	0,1	0,1
$\mathbf{I_{sc}}$	(3.35)	$I_{sc} = I_{D1}$	(3.35)
$\mathbf{V_{oc}}$	V_{D3}	V_{D3}	V_{D3}
$\mathbf{D_{mp}}$	$D_{mp} = 1 - \sqrt{\frac{R_{mp}}{R_L}}$	$D_{mp} = \sqrt{\frac{R_L}{R_{mp}}}$	$D_{mp} = \frac{\sqrt{\frac{R_L}{R_{mp}}}}{1+\sqrt{\frac{R_L}{R_{mp}}}}$

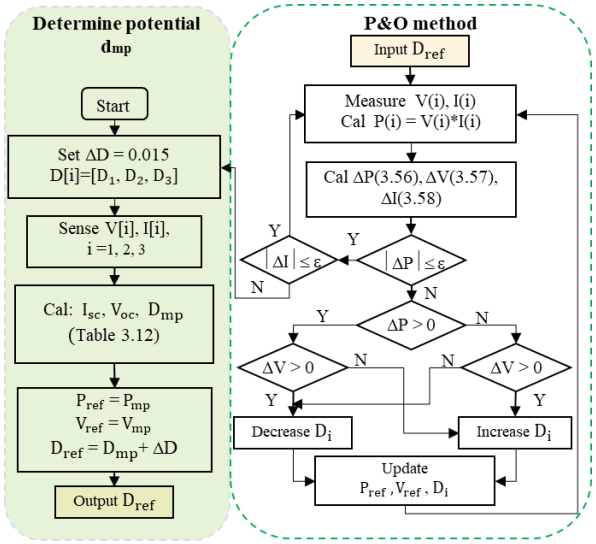

Figure 3.9 Proposed algorithm flowchart.

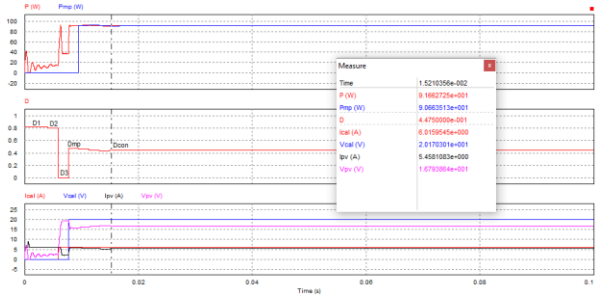

Figure 3.10 Output waveforms using Boost converter under PSC

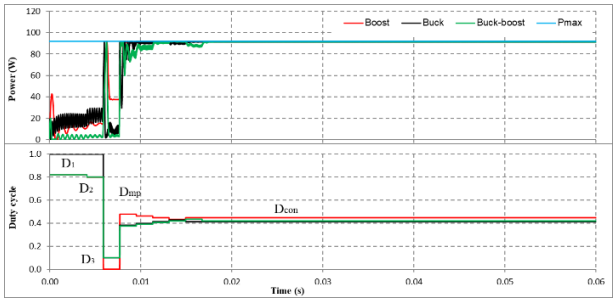

Figure 3.11 MPPT results under PSC (case 7).

3.5.2. Evaluation of efficiency and convergence speed

The data obtained from Table 3.14 shows that:

For the Boost converter, the fastest convergence speed is 0.015 s. The average MPPT efficiency is about 99.27%.

For the Buck converter, the average speed is about 0.0165 s. The average efficiency is about 99.31%.

The Buck-boost circuit's convergence speed is stable at about 0.017 s, and the average efficiency is about 99.27%.

3.5.3. Comparison of efficiency with traditional algorithms

The simulation results compared with the two algorithms, P&O and VSSP&O, show that.

For the Boost converter, the proposed solution reduced the number of iterations by 85% compared with P&O and 80% compared with VSSP&O. Therefore, its convergence speed is the fastest at 0.015 s, while the search times of P&O and VSSP&O are 0.070 s and 0.025 s, respectively.

The Buck converter has the fastest speed of 0.016 s compared with P&O, which is about 0.067 s, and VSSP&O is about 0.021 s. It also reduces the number of iterations by 83% compared with P&O and 73% compared with VSSP&O.

The Buck-boost set reduces the number of iterations by 75% compared with VSSP&O and 82% compared with P&O. The average MPPT times of the proposed algorithm, P&O and VSSP&O are 0.017 s, 0.054 s and 0.026 s, respectively.

Table 3.17. Compare the effectiveness of some recent solutions.

Algorithms	I_P&O	PSO+InC [27]	PSO+P&O [27]	LBNS [28]	CSA [29]	GWO [29]
Convergence speed (s)	0,015	0,0434	0,0495	0,038	0,48	0,19
MPPT Efficiency (%)	100	99,4	99	99,98	99,9	99,99
Algorithms	MIC [29]	PSO [29]	MC-P&O [30]	AFO [22]	COA-FLC [31]	MGWO-ANFIS [32]
Convergence speed (s)	0,014	0,92	0,0375	0,88	0,016	0,02
MPPT Efficiency (%)	99,9	99,96	99,54	98,60	99,83	98,20

3.5.4. Experimental results based on the proposed algorithm

The same scenario is tested with the Chroma 62050H-600S simulator.

The efficiency of the proposed solution with Boost, Buck, and Buck-Boost converters is 99.07%, 99.22%, and 99.51%, respectively. The maximum efficiency can reach 99.95%, the lowest efficiency is around 98.33, and the average efficiency is above 99%.

The D value of the DC/DC converters ranges from 0.41 to 0.81. It ensures that there is no deviation too far from the D = 0.5 to achieve the best efficiency for the DC/DC converter. The solution can be widely applied in small and medium PV systems.

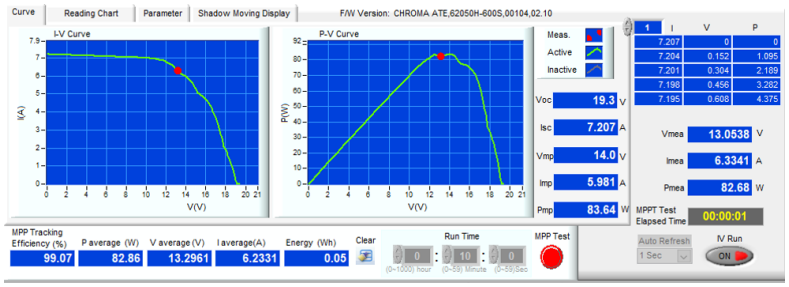

a)

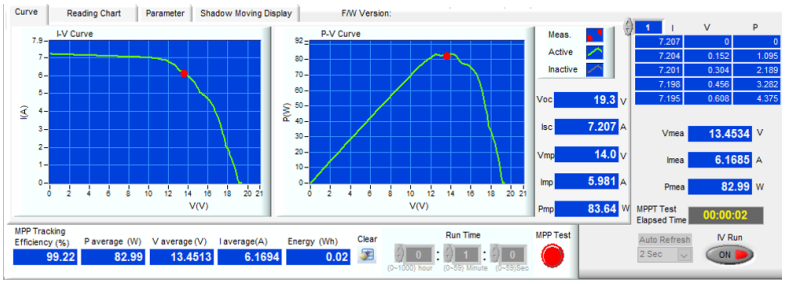

b)

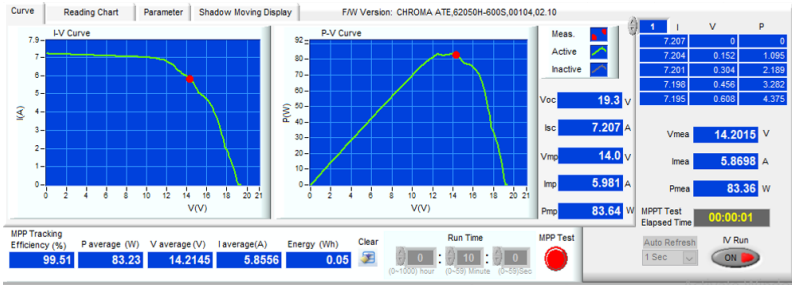

c)

Figure 3.14 MPPT results when experimenting with a) Boost, b) Buck and c) Buck-boost.

3.6. Conclusion of Chapter 3

This chapter proposed a voltage limit of 0.4Voc to improve the starting position for the P&O algorithm. The solution was applied to MPPT for the PV system with parallel configuration in PSC. The results showed it had the highest dynamic response of about 100% at a speed of 0.015s. The potential MPP was calculated accurately, so the search area was limited, reducing the computational burden and improving performance. Specifically, the number of iterations decreased by 76.60% compared to P&O and 69.01% compared to VSSP&O. As a result, the search time was reduced by 71.39% and 21.94%. As a result, the average MPPT efficiency increased by 4.46% compared to the unimproved version and increased by 1.65% compared to VSSP&O. In addition, the I-V characteristic curves of some typical PV types were surveyed with a DC/DC converter. A solution is proposed to calculate the I_{sc} and V_{oc} of PVS without interrupting the power supply. It has the potential for comprehensive and reliable application in MPPT technical solutions. These techniques have been studied, applied, and published in publications {1}, {2}, and {5}.

CHAPTER 4

GMPPT SOLUTION FOR PV SYSTEM WITH SERIAL CONFIGURATION

4.1. Introduction

The parallel configuration is suitable for low-voltage and power applications [33]. In larger systems, S-PC is favored for its flexibility in regulating output voltage and current, but it is necessary to distinguish between GMPPs and LMPPs generated by PSC in the series link [34].

To overcome the above shortcomings, MPPT techniques based on optimization algorithms or hybrid solutions have impressive capabilities in avoiding LMPP traps but are computationally complex, expensive, difficult to implement, and have slow convergence speeds [35]. Meanwhile the hybrid algorithms [36] can combine raditional algorithms' advantages with modern algorithms' accuracy. However, it is necessary to disconnect the power supply to measure I_{sc} and V_{oc}, which leads to large losses. To overcome the above shortcomings, Section 4.3 proposes a GMPPT solution based on the ability to simulate I-V characteristics when PSC occurs.

4.2. Research background

4.2.1. Open circuit voltage of PV system under partial shading conditions

The open circuit voltage of a PV ($V_{oc[i]}$) in a string consisting of N panels in series can be calculated by dividing the open circuit voltage of the string ($V_{oc,sys}$) by the number of PVs [37].

$$V_{oc[i]} = i\frac{V_{oc,sys}}{N};\ i = 1 \text{ to } N \qquad (4.1)$$

The voltage at the MPP (M_1 in Figure 4.1) is proportional to $V_{oc[i]}$ by the factor k_v as in Eq. (4.2) [38]. Previous solutions rely on this relative distance to scan the entire I-V curve. This study proposes a solution to determine the voltage gap between two points, B and B' (in Figure 4.1), to calculate $V_{mp[2]}$. Accurately estimated MPP locations are the basis for improving the MPPT performance of PV systems using small adjustment steps.

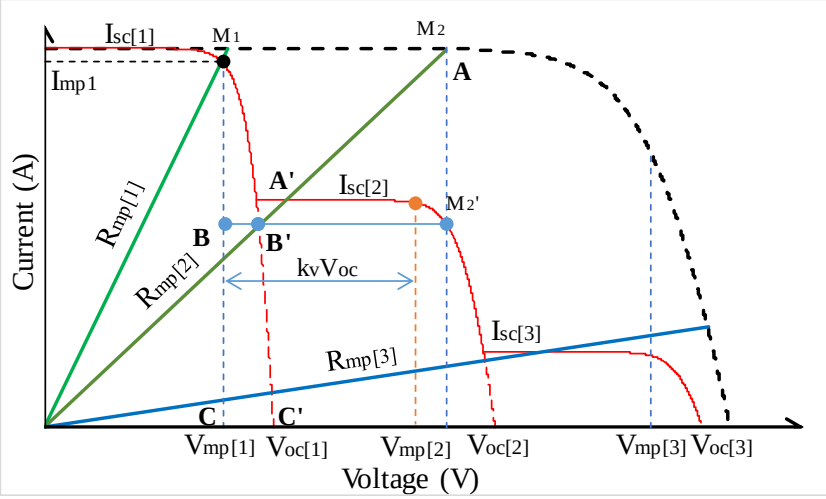

Figure 4.1 Voltage region on I-V curve under partial shade conditions.

$$V_{mp[1]} = k_v\frac{V_{oc,sys}}{N} \qquad (4.2)$$

4.2.2. Short-circuit current of PV system under partial shading conditions

The disadvantage of the CV and CC method is that the power supply must be interrupted to measure I_{sc} and V_{oc}, reducing power generation efficiency. Section 3.2 proposes a solution to measure I_{sc} according to the operating conditions for the DC/DC converter. This method can also be found in [39]. Therefore, the basic parameters of the PVS can be measured directly according to D without interrupting the power supply.

4.3. Proposed GMPPT solution based on the I-V curve under PSC

4.3.1. Determine MPP in the first interval on the I-V curve

a. Open circuit voltage of the first PV on the I-V curve

The block diagram of the PV system using a Buck-boost converter is shown in Figure 4.2. The value of $V_{oc,sys}$ is measured directly at D = 0.1, and then equations (4.1) and (4.2) are applied to calculate the voltage at the first extreme peak with $k_v = 0.8$. This method has been demonstrated in Section 3.3 and published in publications {1} and {2}.

b. Short circuit current of the first PV on the I-V curve

The characteristic of series configuration is that the short circuit current of the PV system, $I_{sc,sys}$, is also the short circuit current of the PV receiving the most energy. Therefore, the value of $I_{sc[1]} = I_{sc,sys}$ when setting the initial parameter D = 0.8.

In summary, set $D_1 = 0,8$ and $D_2 = 0,1$ to measure $I_{sc,sys}$ and $V_{oc,sys}$, then calculate the first MPP at M_1 as follows:

$$V_{mp[1]} = k_v V_{oc[1]} = k_v \frac{V_{oc,sys}}{N} \tag{4.3a}$$

$$I_{mp[1]} = k_i I_{sc[1]} = k_i I_{sc,sys} \tag{4.3b}$$

The internal resistance of PV at position M_1 is.

$$R_{mp[1]} = \frac{V_{mp[1]}}{I_{mp[1]}} \tag{4.4}$$

Determine $D_{mp[1]}$ at M_1 according to the following (4.5).

$$D_{mp[1]} = \frac{\sqrt{\frac{R_L}{R_{mp[1]}}}}{1+\sqrt{\frac{R_L}{R_{mp[1]}}}} \tag{4.5}$$

With the calculated $D_{mp[1]}$ value, update the M_1 coordinates into the table of potential MPP values.

4.3.2. Determine the remaining MPPs in the PV system

a. Determine the Vmp value at the LMPPs

The voltage at B' is calculated approximately when considering two similar triangles, M_1BB' and M_1CC', as follows:

$$V_{B'} - V_{mp[1]} = (1-k_v)V_{oc[1]} \frac{k_i(I_{sc[1]} - I_{sc[2]})}{k_i I_{sc[1]}} = (1-k_v)V_{oc[1]} \frac{I_{sc[1]} - I_{sc[2]}}{I_{sc[1]}} \tag{4.6}$$

So the voltage at B' is

$$V_{B'} = (1-k_v)V_{oc[1]} \frac{I_{sc[1]} - I_{sc[2]}}{I_{sc[1]}} + V_{mp[1]} \tag{4.7}$$

The position of $V_{mp[2]}$ coincides with $M_{2'}$ and differs from B' by a distance of $k_v V_{oc[1]}$, so $V_{mp[2]}$ is calculated according to equation (4.8).

$$V_{mp[2]} = V_{B'} + k_v V_{oc[1]} = V_{mp[1]} + V_{oc[1]} \left[(1-k_v) \frac{I_{sc[1]} - I_{sc[2]}}{I_{sc[1]}} + k_v \right] \tag{4.8}$$

The $V_{mp[2]}$ value calculated in this way is more accurate than updating an interval $V_{mp[2]} = V_{mp[1]} + k_v V_{oc[1]}$ in previous studies.

In general, the value of $V_{mp[i]}$ in a PV system with N PV panels connected in series under partial shading conditions is determined by equation (4.10) with i = 2 to N.

$$V_{mp[i]} = V_{mp[i-1]} + V_{oc[1]} \left[(1-k_v) \frac{I_{sc[i-1]} - I_{sc[i]}}{I_{sc[i-1]}} + k_v \right] \tag{4.10}$$

b. Determine the Imp value at the LMPPs

On the I-V curve (Figure 4.1), the value of $V_{mp[2]}$ calculated by formula (4.10) is also the voltage at two points, M_2 and $M_{2'}$. Therefore, the resistance value R_{mp2} is determined by equation (4.11):

$$R_{mp[2]} = \frac{V_{mp[2]}}{I_{sc[1]}} \quad (4.11)$$

Calculate $D_{mp[2]}$ according to equation (4.5), then measure and check the voltage at $D_{mp[2]}$ to confirm the shade according to the following principle:

b1. If $V_{mp[1]} < V_{A'} < V_{oc[1]}$ there is shading on the PV system and $I_{sc[2]} << I_{sc[1]}$ so the measured current $I_{sc[2]} < I_{A'} < I_{sc[1]}$. Therefore, $V_{A'}$ must be increased by adjusting $D_{mp[2]}$ through adjusting $R_{mp[2]}$ according to equation (4.12) until $V_{A'} > V_{oc[1]}$.

$$R_{mp[2]} = R_{mp[2]} + \lambda \frac{V_{oc[1]}}{I_{sc[1]}} \quad (4.12)$$

b2. If $V_{oc[1]} < V_{A'} < 1.4V_{oc[1]}$, there is shading on the PV system and $I_{sc[2]} = I_{A'}$, the MPP point to be determined is M2', as shown in Figure 4.1. With $I_{sc[2]} = I_{A'}$, recalculate the values of $R_{mp[2]}$ and $D_{mp[2]}$ to update the current position. Check the remaining PVs following the same steps.

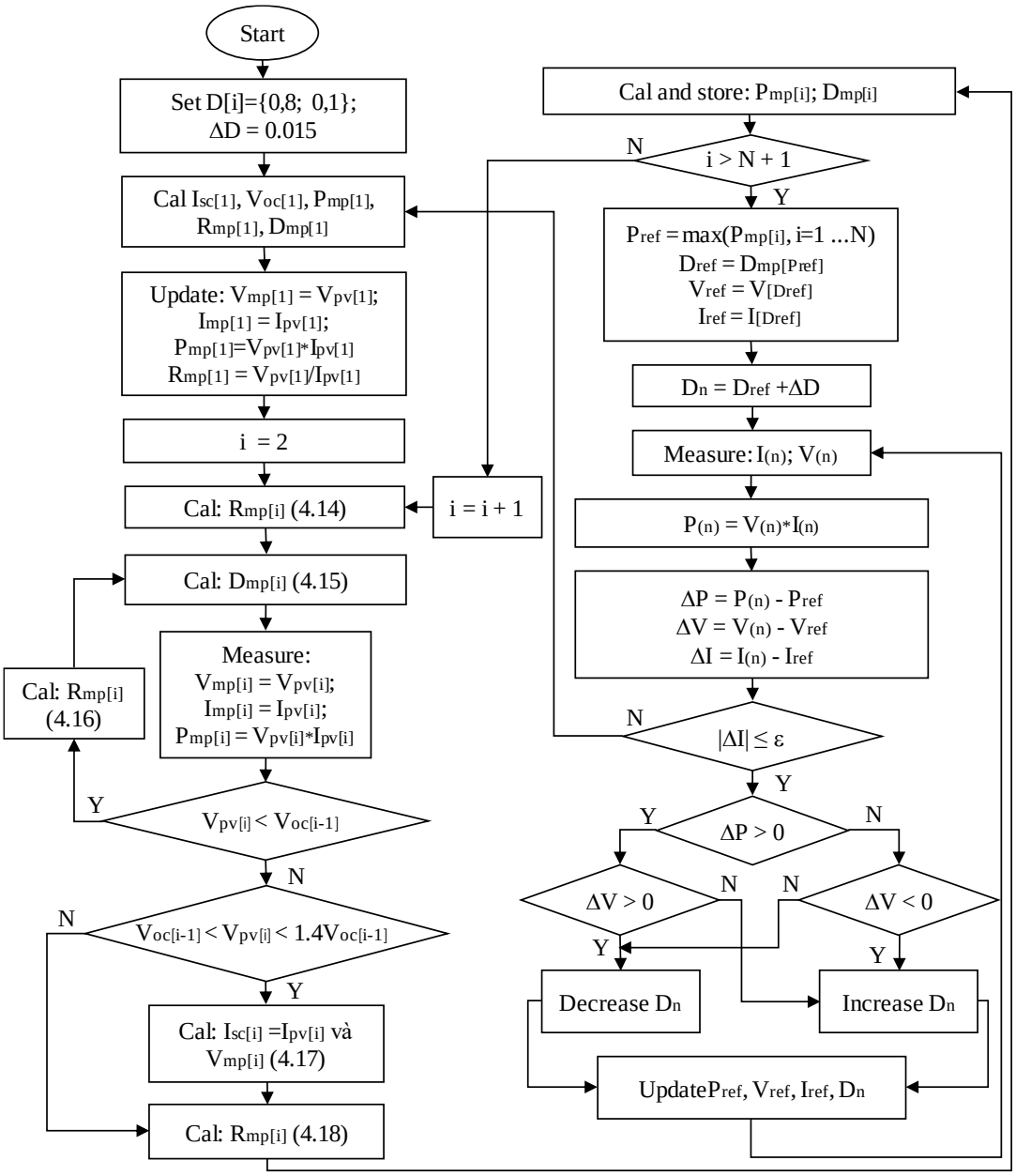

Figure 4.2 Proposed GMPPT algorithm flowchart.

b.3. If $V_{A'} > 1.4V_{oc[1]}$, there is no shading on the PV system and $I_{sc[1]} = I_{sc[2]}$. Select $I_{sc[2]} = I_{A'}$, recalculate the value of $R_{mp[2]}$ and update $D_{mp[2]}$.

$$R_{mp[2]} = \frac{V_{mp[2]}}{k_i I_{sc[2]}} \quad (4.13)$$

Checking the final PV, the GMPP region has the largest P_{mp} among the stored $P_{mp[i]}$. These are reference points for

applying the P&O method for accurate convergence point checking.

4.3.3. Proposed GMPPT algorithm flowchart

The GMPPT algorithm flowchart of the PV system under partial shading conditions is shown in Figure 4.3.

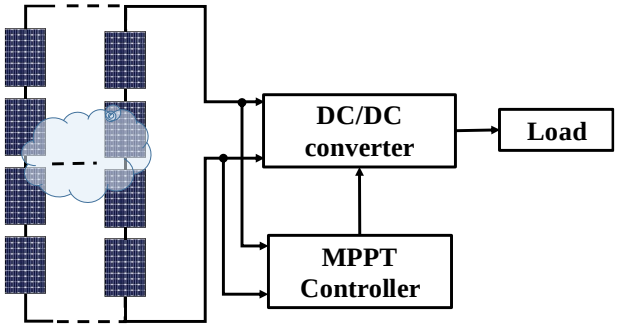

Figure 4.3 Proposed PV system structure.

4.3.4. Applications and results achieved

The proposed simulation cases listed in Table 4.1 focus on the following objectives:

- Simulate the response of the proposed algorithm with a string of 4 PV panels under partial shading operating conditions.
- Simulate and verify the algorithm's response under partial shading conditions when multiple strings are parallel.
- Compare the dynamic response of the proposed algorithm with two other optimization algorithms, PSO and GA, under the same stable and continuously changing operating conditions.
- Experiment with partial shading conditions on a PV string through a Chroma simulator.

The structure of the PV system applied for the proposed solution in this study is shown in Figure 4.3.

Table 4.1. Simulation cases with the proposed algorithm.

Cases		Irradiation (W/m^2)				Number of MPP	GMPP locations	P_{max} (W)
		PV1	PV2	PV3	PV4			
1		500	500	500	500	1	1	116,51
2		700	500	400	200	4	3	77,20
3		600	500	400	300	4	4	78,62
4		1000	200	300	400	4	1	59,88
5		950	750	300	250	4	2	94,74
6		950	200	250	350	4	1	56,80
7		800	700	600	300	4	3	115,03
8		900	500	250	100	4	2	64,29
9	String 1	1000	1000	1000	1000	1	1	479,72
	String 2	1000	1000	1000	1000			
10	String 1	1000	900	400	750	4	2	247,98
	String 2	800	450	1000	500			
11	String 1	500	1000	700	1000	3	1	280,11
	String 2	1000	700	1000	500			
12	String 1	1000	1000	400	400	2	2	242,12
	String 2	400	400	1000	1000			
13	String 1	1000	900	450	200	4	3	311,71
	String 2	200	700	450	900			
	String 3	900	200	400	100			

a. Simulation with a PV string

Under uniform or full shade conditions, the proposed algorithm always finds GMPP in less than 22 ms after calculating the values of $I_{sc,sys}$, $V_{oc,sys}$, and $D_{mp[i]}$ in 15 ms (Figure 4.5). The algorithm needs 4 adjustment steps to converge at D_{mp}. The estimated power at $D_{mp[4]}$ is $P_{mp[4]}$ = 116,40 W, achieving an efficiency of about 99,98%.

Under partial shading conditions, the $P_{mp[1]}$ value is approximately $P_{mp[3]}$ (Figure 4.6). The $D_{mp[i]}$ and $P_{mp[i]}$ values are calculated in about 15.7 ms and through 4 adjustment steps to converge at D_{mp} = 0,0595 with a total time of about 28 ms. The stable power is about 59.83 W, reaching 99.92%. All simulation cases have an efficiency above 99%, with an average value of 99.70%.

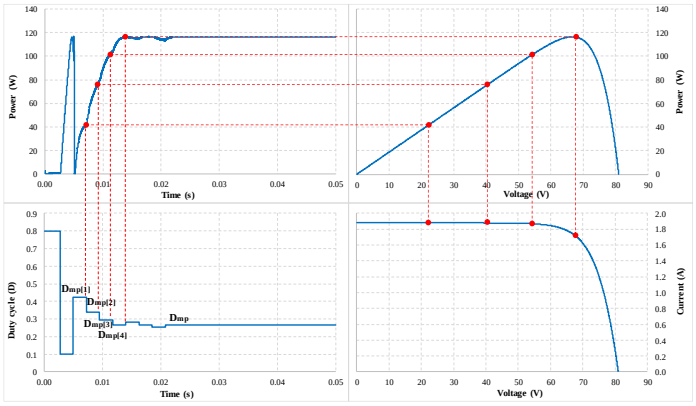

Figure 4.5 Output waveform when simulated under uniform conditions.

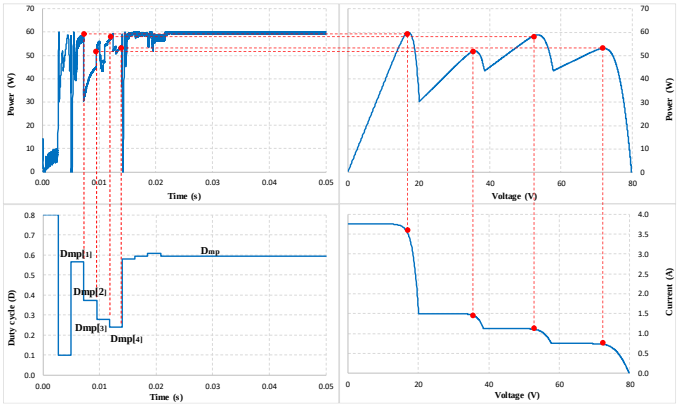

Figure 4.6 Output waveform when simulated under partial shade conditions.

b. Simulation with multiple parallel PV strings

The investigated cases include two or three parallel strings operating under uniform or partial shading conditions. Figure 4.8 shows the power waveform and the duty cycle D when operating three strings under PS conditions. The results show that when $I_{sc,sys}$ and $V_{oc,sys}$ are determined from the two initial D values, four D values are deployed to search in different ranges. The total time from start-up to convergence at the working position is about 0.027 s, with the amount of power generated reaching 99.94% of the maximum power of the PV system. This result also shows that although the increase in the number of parallel strings means an increase in the $I_{sc,sys}$ current, the solution is still capable of effectively avoiding LMPP traps and accurately extracting the GMPP value of the PV system. It can be explained in detail that the two particular positions on the I-V curve have been limited, so the solution only searches for LMPPs within the predetermined range without drifting out of the potential region. Moreover, the solution only increases the number of calculations without increasing the number of iterations, so the PV system stabilizes sooner than previous techniques.

The synthesis of all simulation cases shows that the convergence speed ranges from 21 ms to 32 ms. All simulation cases have an efficiency above 99%, with an average value of about 99.68%. It shows that the proposed method can accommodate a variety of PV configurations and operate under different conditions.

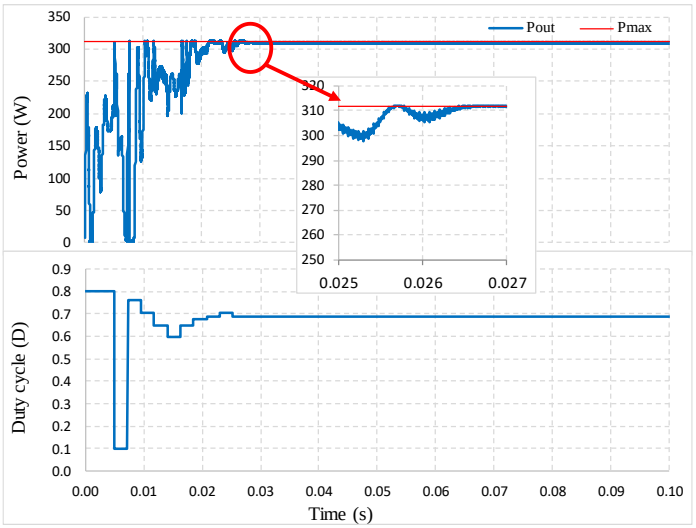

Figure 4.8. Output waveform when simulating 3 parallel strings under PSC.

c. Comparison of dynamic response with optimization algorithms

When compared with other algorithms under partial shading conditions (Figure 4.9), the proposed solution only takes 18.8 ms to stabilize the output power and achieves an efficiency of 99.92% compared with 99.97% of GA in 82 ms and 98.58% of PSO in 70 ms. The average efficiency of the proposed solution is 99.70% compared with 98.67% of PSO and 98.09% of GA. The proposed algorithm's convergence speed is the fastest, averaging about 19.97 ms, compared with 67.5 ms of PSO and 52.25 ms of GA (Table 4.2).

Table 4.2. Summary of MPPT efficiency and convergence speed of algorithms.

Cases	P_{max} (W)	P_{out} (W)			Efficiency (%)			Convergence speed (ms)		
		Proposed	PSO	GA	Proposed	PSO	GA	Proposed	PSO	GA
1	116,51	116,40	113,98	116,41	99,91	97,83	99,91	21	75	36
2	77,20	77,07	76,22	75,49	99,83	98,73	97,78	27	75	46
3	78,62	78,21	75,58	75,05	99,48	96,13	95,46	27	74	58
4	59,88	59,83	59,03	59,86	99,92	98,58	99,97	28	70	82
5	94,74	94,11	94,59	92,37	99,34	99,84	97,50	31	62	51
6	56,80	56,53	56,54	53,69	99,52	99,54	94,52	23	69	66
7	115,03	115,01	114,83	114,64	99,98	99,83	99,66	28	57	41
8	64,47	64,20	63,77	63,65	99,58	98,91	98,73	31	58	38
Average value					99,70	98,67	97,94	27	67,5	52,25

Under the continuous change conditions (Figure 4.10), the proposed solution and GA stabilize almost simultaneously at 0.430s, while the PSO algorithm takes 0.510s. Overall, the average performance increased by 0.99% compared to PSO and 3.45% compared to GA. Meanwhile, the average search time decreased by 70.4% and 61.77%, respectively.

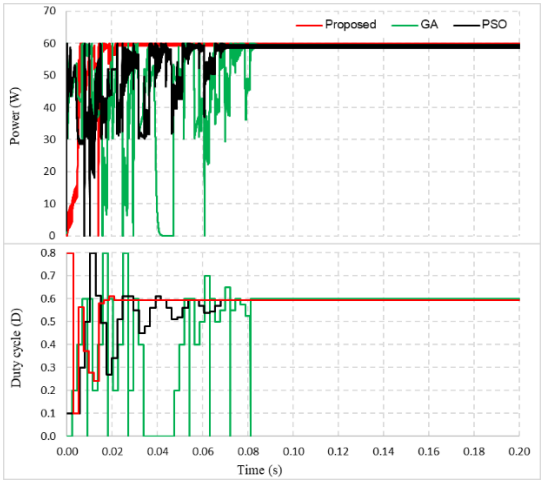

Figure 4.9 Compare the output waveforms of the algorithms under PSC.

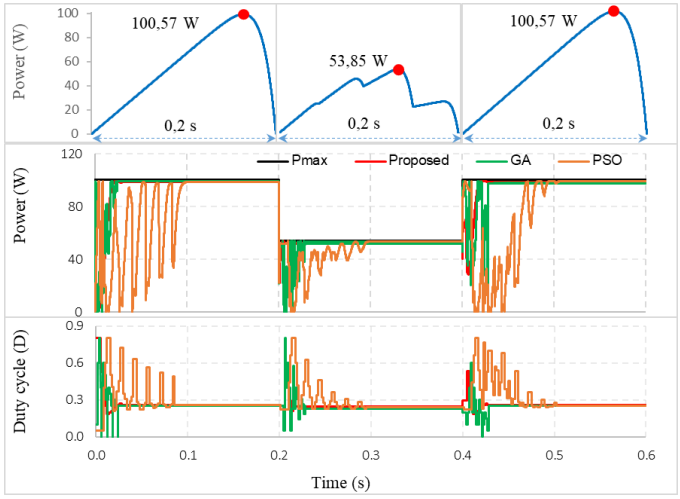

Figure 4.11 Comparison of GMPP performance under PSC is continuously varied.

d. Experimental results

Under uniform conditions, the MPPT efficiency is about 99.95% (Figure 4.13a) and slightly decreases when partial shading occurs (Figure 4.13b), approximately 98.59%; the average value is about 99.13%.

In summary, $I_{sc,sys}$ and $V_{oc,sys}$ are calculated based on D to locate LMPPs on the I-V characteristic curve. The proposed solution accurately calculates the voltage deviation between two consecutive MPP positions. This increase the speed and MPPT efficiency compared to other optimization algorithms under the same test conditions. The results have confirmed that

this method is capable of effectively avoiding LMPP trapping based on the operating principle in Section 4.3.2. It is a simpler, easier to implement, and more reliable solution under partial shading conditions by automatically adjusting the ΔV and ΔR according to the operating conditions while ΔD is selected with a small and fixed value to increase the efficiency and stability around the GMPP point. It can be applied in series-connected or S-PC PV systems operating under different conditions considering the influence of bypass diodes.

4.4. Conclusion of Chapter

The content of Chapter 4 proposes a GMPPT solution for the SC or S-PC coupled PV system under partial shading conditions, as shown in the following application studies.

Inheriting and promoting the proposal of an operating range of less than 0.4Voc from Chapter 3 to locate LMPPs in the step region on the I-V characteristic curve caused by partial shading. Developing a solution to directly determine the $I_{sc,sys}$ and $V_{oc,sys}$ of a PV system consisting of one or several parallel strings based on simulation of their operating curves. In addition, the proposed solution accurately calculates the voltage error between two consecutive extreme peaks on the I-V characteristic curve when PSC occurs, and adjusting the operating region according to ΔR has reduced the number of loops for the P&O algorithm to reduce the number of search iterations. The results confirmed the GMPPT capability of the proposed algorithm is better than the optimization algorithms under the same operating conditions. Specifically, the proposed algorithm has reduced 70.4% of the calculation time compared to PSO and 61.77% compared to GA. Therefore, efficiency increased by 0.98% and 3.32%, respectively. It contributes to clarifying the GMPPT technique based on the ability to simulate the operating state of a PV system under actual operating conditions. Therefore, the proposed algorithm has a lot of potential for application in PV systems operating under different conditions, especially partial shading. This proposed solution has been studied and applied in the published work No. {3} and related work No. {6-9}.

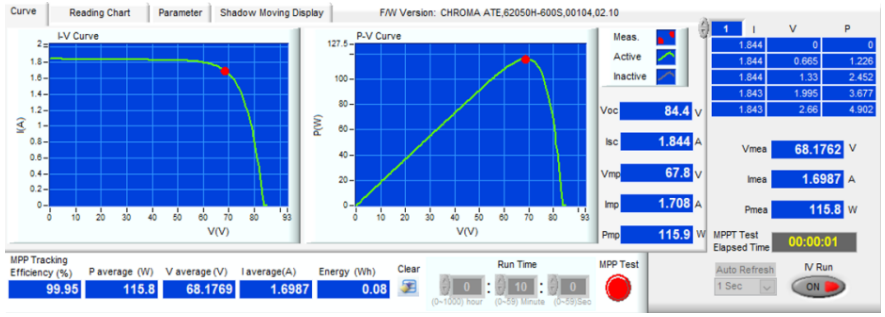

Figure 4.13 Experimental results under a) uniform conditions, b) PSC

CHAPTER 5. CONCLUSION

5.1. Achievements

The thesis "**Improving the efficiency of photovoltaic systems**" has studied, analyzed, and proposed MPPT techniques to improve the efficiency of energy exploitation from PV systems. The outstanding advantages of the proposed method are its simple structure, easy implementation, high MPPT efficiency, and reduced number of iterations compared to previous traditional and improved versions. The focus of the thesis has solved two MPPT problems derived from the proposed solutions, including:

5.1.1. MPPT solution for PV systems with parallel cofiguration

The thesis has proposed an MPPT algorithm for parallel PV systems operating in partial shade conditions. The main contribution of this solution is the proposal of a voltage limit in the region of $0.4V_{oc}$ to quickly estimate the starting position for the improved P&O algorithm. Based on the proposed solution, a series of PVs belonging to three groups, monocrystalline, polycrystalline, and thin-film, were investigated for their output characteristics under the impact of the working environment. This work investigate the linear and nonlinear regions on the I-V curve to directly calculate the I_{sc} and V_{oc} of the PV system by extrapolation without interrupting the power supply. In addition, the Boost, Buck, and Buck-boost converters were also investigated for their optimal operating limits to find the best D value under each working condition. Combining of these two steps has helped to quickly and accurately locate the MPP region of the PV system. Therefore, the proposed solution must only re-check the accuracy using a simple P&O algorithm to increase the MPPT efficiency. The simulation and experimental results on the PV system in parallel connect show that it has the highest dynamic response capability of up to 100% in 0.015 s. In addition, the MPPT capability of this algorithm is also directly compared with the traditional P&O version and VSSP&O. The proposed solution has an average number of iterations reduced by 76.60% compared with P&O and 69.01% compared with VSSP&O. Therefore, the calculation time has been reduced by 71.39% and 21.94%, respectively. Additionally, the average MPPT efficiency has improved by 4.46% compared with the unimproved version and 1.65% compared with VSSP&O. It has excellent potential for application in PV systems with medium and small capacity. This proposed method has been implemented and published in works {1}, {2} and {5}.

5.1.2. Proposing GMPPT solution for PV system with series-connected

Kế Based on the results obtained from the proposal in Chapter 3, the thesis continues to improve the traditional P&O algorithm to GMPPT for systems consisting of PVs connected in series or multiple PV strings connected in parallel. The method of simulating the I-V curve under partial shading conditions to determine GMPP is used. The thesis has proposed to improve two key issues to increase the ability to quickly and accurately estimate the GMPP area among LMPPs. Firstly, the parameters $I_{sc,sys}$ and $V_{oc,sys}$ of the PV system are determined directly from the most favorable locations to avoid power interruption and are more accurate than the CC or CV method. Secondly, a method is proposed to determine the voltage deviation between consecutive MPP peaks when partial shading occurs. This work is inherited from the proposal of a voltage limit of less than $0.4V_{oc}$ in the previous study to determine the shading state quickly. In this way, the proposed solution will reduce the calculation error because it considers the conditions. The above two improvements help to estimate MPP faster with smaller errors. This increases the search speed and improves the power generation efficiency of the PV system. The comparison results with two optimal algorithms under the same working conditions show that the proposed algorithm has reduced the calculation time by 70.4% compared to PSO and 61.77% compared to GA. Therefore, efficiency increased by 0.98% and 3.32%, respectively. The proposed method has great potential for application in PV systems with series

configuration or S-PC with outstanding efficiency and speed. The proposals in this research content have been applied and published in work number {3} and related works number {4}, and {6 - 9}.

5.2. Future work

Although the thesis has achieved some reliable research results in applying MPPT technology to improve the power generation efficiency of PV systems. However, there are still some limitations. In the following studies, the author continues to apply the achieved results to improve the limitations:

- Building a GMPPT algorithm in partial shading conditions considering other influencing factors besides radiation and surface temperature.
- Proposing high-step-up configurations, improving the quality of dynamic stability around the MPP point of the PV system in partial shading conditions.
- Determining the fault area in the PV string under actual working conditions based on the output characteristics of the PV system.

REFERENCES

[1] I. Iam, Z. Ding, Z. Huang, C. Lam, R. Martins und P. Mak, „A Flexible Rooftop Photovoltaic-Inductive Wireless Power," *IEEE Access,* Bd. 11, p. 51117–51132, 2023.

[2] H. Farh, A. Fathy, A. Al-Shamma'a, S. Mekhilef und A. Al-Shaalan, „Global research trends on photovoltaic maximum power extraction:," *Sustainable Energy Technologies and Assessments,* Bd. 61, p. 103585, 2024.

[3] A. Baba, G. Liu und X. Chen, „Classification and Evaluation Review of Maximum Power Point Tracking Methods," *Sustainable Futures,* Bd. 2, p. 100020, 2020.

[4] L. Gao, R. A. Dougal, S. Liu und A. P. Iotova, „Parallel-Connected Solar PV System to Address Partial and Rapidly Fluctuating Shadow Conditions," *IEEE Transactions on Industrial Electronics,* Bd. 56, Nr. 5, pp. 1548 - 1556, 2009.

[5] R. K. Pachauri, O. P. Mahela, A. Sharma, J. Bai, Y. K. Chauhan, B. Khan und H. H. Alhelou, „Impact of partial shading on various PV array configurations and different modeling approaches: A comprehensive review," *IEEE Access,* Bd. 8, pp. 181375-181403, 2020.

[6] C. L. F. Belhachat, „Modeling, analysis and comparison of solar photovoltaic array configurations under partial shading conditions," *Solar Energy,* Bd. 120, p. 399–418, 2015.

[7] S. A. S. R. W. M. K Abdulmawjood, „Characteristic study of solar photovoltaic array under different partial shading conditions," *IEEE Access,* Bd. 10, pp. 6856 - 6866, 2022.

[8] D. Khodair, S. Motahhir, H. Mostafa, A. Shaker, H. Munim, M. Abouelatta und A. Saeed, „Modeling and Simulation of modified MPPT techniques under varying operating climatic conditions," *Energies,* Bd. 16, Nr. 1, p. 549, 2023.

[9] M. Katche, A. Makokha, S. Zachary und M. Adaramola, „A Comprehensive Review of Maximum Power Point Tracking (MPPT) Techniques Used in Solar PV Systems," *Energies,* Bd. 16, p. 2206, 2023.

[10] S. Bhattacharyya, S. Samanta und S. Mishra, „Steady Output and Fast Tracking MPPT (SOFT-MPPT) for P&O and InC Algorithms," *IEEE Transactions on Sustainable Energy,* Bd. 12, Nr. 1, pp. 293 - 302, 2021.

[11] A. A. R. M. A. S. O. M Lasheen, „Adaptive reference voltage-based MPPT technique for PV applications," *IET Renewable Power Generation,* Bd. 11, Nr. 5, pp. 715-722, 2017.

[12] B. A. Y. D. I Dagal, „A modified multi-stepped constant current based on gray wolf algorithm for photovoltaics applications," *Electrical Engineering,* pp. 10.1007/s00202-023-02180-z, 2024.

[13] A. Baatiah, A. Eltamaly und M. Alotaibi, „Improving Photovoltaic MPPT Performance through PSO Dynamic Swarm Size Reduction," *Energies,* Bd. 16, p. 6433, 2023.

[14] C. González-Castaño, C. Restrepo, S. Kouro und J. Rodriguez, „MPPT Algorithm Based on Artificial Bee Colony for PV System," *IEEE Access,* Bd. 9, pp. 43121 - 43133, 2021.

[15] V. R. S. P. F. A. N Priyadarshi, „An ant colony optimized MPPT for standalone hybrid PV-wind power system with single Cuk converter," *Energies,* Bd. 12, Nr. 1, p. 167, 2019.

[16] S. B. S. M. M. I. S. M. NI Nahin, „A modified PWM strategy with an improved ANN based MPPT algorithm for solar PV fed NPC inverter driven induction motor drives," *IEEE Access,* Bd. 11, pp. 70960 - 70976, 2023.

[17] M. Shehab, M. Abu-Hashem, M. Shambour, A. Alsalibi, O. Alomari, J. Gupta, A. R. Alsoud, B. Abuhaija und L. Abualigah, „A Comprehensive Review of Bat Inspired Algorithm: Variants, Applications, and Hybridization," *Archives of Computational Methods in Engineering,* Bd. 30, pp. 765-797, 2023.

[18] E. Y. İ Yazıcı, „Modified grey wolf optimizer based MPPT design and experimentally performance evaluations for wind energy systems," *Engineering Science and Technology,* Bd. 46, p. 101520, 2023.

[19] K. C. T. L. KH Huang, „An improved photovoltaic module array global maximum power tracker combining a genetic algorithm and ant colony optimization," *Technologies,,* Bd. 11, Nr. 2, p. 61, 2023.

[20] A. Dawahdeh, H. Sharadga und S. Kumar, „Novel MPPT Controller Augmented with Neural Network for Use with Photovoltaic Systems Experiencing Rapid Solar Radiation Changes," *Sustainability,* Bd. 16, p. 1021, 2024.

[21] A. L. A. B. R. H. H. C. A. M. I. S. M. M. S Abboud, „Optimizing Solar Energy Production in Partially Shaded PV Systems with PSO-INC Hybrid Control," *Journal of Robotics and Control,* Bd. 5, Nr. 2, pp. 312-320, 2024.

[22] Y. L. B. Z. K Xia, „Improved Photovoltaic MPPT Algorithm Based on Ant Colony Optimization and Fuzzy Logic Under Conditions of Partial Shading," *IEEE Access,* Bd. 12, pp. 44817-44825, 2024.

[23] Z. S. J Ahmed, „An enhanced adaptive P&O MPPT for fast and efficient tracking under varying environmental conditions," *IEEE Transactions on Sustainable Energy,* Bd. 9, Nr. 3, pp. 1487 - 1496, 2018.

[24] F. W. F Yi, „Review of voltage-bucking/boosting techniques, topologies, and applications," *Energies,* Bd. 16, Nr. 2, p. 842, 2023.

[25] T. R. Kandipati Rajani, „Reconfiguration of PV Arrays (T-C-T, B-L, H-C) Considering Wiring Resistance," *CSEE Journal of Power and Energy Systems,* Bd. 8, Nr. 5, pp. 1408 - 1416, 2022.

[26] A. D. G. A Orioli, „A procedure to calculate the five-parameter model of crystalline silicon photovoltaic modules based on the tabular performance data," *Applied energy,* Bd. 102, p. 1160–1177, 2013.

[27] M. Ibrahim, S. Ang, M. Dani, M. Rahman, R. Petra und S. Sulthan, „Optimizing Step-Size of Perturb & Observe and Incremental Conductance MPPT Techniques Using PSO for Grid-Tied PV System," *IEEE Access,* Bd. 11, p. 13079, 2023.

[28] C. A. Y. M. I Pervez, „A Reduced Search Space Exploration Metaheuristic Algorithm for MPPT," *IEEE Access,* Bd. 10, pp. 26090 - 26100, 2022.

[29] N. Pamuk, „Performance Analysis of Different Optimization Algorithms for MPPT Control Techniques under Complex Partial Shading Conditions in PV Systems," *Energies,* Bd. 16, Nr. 8, p. 3358, 2023.

[30] R. Morales, J. Rohten, M. Garbarino, J. Muñoz, J. Silva, E. Pulido, J. Espinoza und M. Andreu, „A Novel Glob-al MPPT Method Based on Measurement Cells," *IEEE Access* , Bd. 10, pp. 97481-97494, 2022.

[31] S. Zand, S. Mobayen, H. Gul, H. Molashahi, M. Nasiri und A. Fekih, „Optimized Fuzzy Controller Based on Cuckoo Opti-mization Algorithm for Maximum Power-Point Tracking of Photovoltaic Systems.," *IEEE Access,* Bd. 10, pp. 71699-71716, 2022.

[32] C. H. Basha, M. Palati, C. Dhanamjayulu, S. Muyeen und P. Venkatareddy, „A novel on design and implementation of hybrid MPPT controllers for solar PV systems under various partial shading conditions," *Scientific Reports,* Bd. 14, p. 1609, 2024.

[33] M. M. R. W. P. M. M. Z. O. I. A Calcabrini, „A fully reconfigurable series-parallel photovoltaic module," *Renewable Energy,* Bd. 179, pp. 1-11, 2021.

[34] R. R. S Malathy, „Comprehensive analysis on the role of array size and configuration on energy yield of photovoltaic systems under shaded conditions," *Renewable and Sustainable Energy Reviews,* Bd. 49, p. 672–679, 2015.

[35] G. H. C. H. L Gong, „A two-stage MPPT controller for PV system based on the improved artificial bee colony and simultaneous heat transfer search algorithm," *ISA transactions,* Bd. 132, pp. 428-443, 2023.

[36] O. B. M. M. A Hassan, „An improved genetic algorithm based fractional open circuit voltage MPPT for solar PV systems," *Energy Reports,* Bd. 9, pp. 1535-1548, 2023.

[37] Z. S. J Ahmed, „An accurate method for MPPT to detect the partial shading occurrence in a PV system," *IEEE transactions on industrial informatics,* Bd. 13, Nr. 5, pp. 2151 - 2161, 2017.

[38] Y. C. H. L. W. T. M. L. J. W. Z. L. L Li, „A Multi-Producer Group-Search-Optimization Method-Based Maximum-Power-Point-Tracking for Uniform and Partial Shading Condition," *IEEE Access,* Bd. 8, pp. 184688 - 184696, 2020.

[39] K. M. S. M. M. M. RI Jabbar, „A modified perturb and observe MPPT for a fast and accurate tracking of MPP under varying weather conditions," *IEEE Access,* Bd. 11, pp. 76166 - 76176, 2023.

[40] Y. M, C. R und G. A, „Enhanced photovoltaic systems performance: Anti-Windup PI controller in ANN-Based ARV MPPT method," *IEEE Access,* Bd. 11, pp. 90498 - 90509, 2023.